RESEARCH ARTICLE `OPEN ACCESS`

Neural Representation Precision of Distance Predicts Children's Arithmetic Performance

Hui Zhao[1] | Wang Qi[1] | Jiahua Xu[2] | Yaxin Yao[1] | Jianing Lyu[1] | Jiaxin Yang[1] | Shaozheng Qin[1,3]

[1]State Key Laboratory of Cognitive Neuroscience and Learning & IDG/McGovern Institute for Brain Research, Beijing Normal University, Beijing, China | [2]Psychiatry Research Center, Beijing Huilongguan Hospital, Peking University Huilongguan Clinical Medical School, Beijing, China | [3]Beijing Key Laboratory of Brain Imaging and Connectomics, Beijing Normal University, Beijing, China

Correspondence: Hui Zhao (huizhao@bnu.edu.cn)

ABSTRACT

Focusing on the distance between magnitudes as the starting point to investigate the mechanism of relation detection and its contribution to mathematical thinking, this study explores the precision of neural representations of numerical distance and their impact on children's arithmetic performance. By employing neural decoding techniques and representational similarity analysis, the present study investigates how accurately the brain represents numerical distances and how this precision relates to arithmetic skills. Twenty-nine school-aged children participated, completing a dot number comparison task during fMRI scanning and an arithmetic fluency test. Results indicated that neural activation patterns in the intra-parietal sulcus decoded the distance between the presented pair of dots, and higher precision in neural distance representation correlates with better arithmetic performance. These findings suggest that the accuracy of neural decoding can serve as an index of neural representation precision and that the ability to precisely encode numerical distances in the brain is a key factor in mathematical abilities. This provides new insights into the neural basis of mathematical cognition and learning.

1 | Introduction

Figuring out the relation between items is fundamental for individuals to acknowledge the world. People organize their travel itineraries by labeling landmarks as near or far to aid in navigation, compare similarities and differences between words to build semantic concepts, and assess familiarity and strangeness in social interactions. Mathematics is not only a fundamental subject in education, but also a scientific discipline that uses quantitative language to describe relations and rules between objects with precision. Learning mathematics from a relational perspective might help students grasp its essence. These relations can be described creatively and universally, such as in Einstein's equation $E = mc^2$, where c^2 represents the relation between E and m. Among these relations, distinguishing magnitudes and recognizing the distances between them is perhaps the simplest and most basic form of relation detection.

The capacity to differentiate magnitudes is considered intuitive and foundational to mathematical cognition and learning (Ansari 2008; Brannon 2006; Dehaene 1992). However, there has not been a study focusing on the representation of distance between magnitudes, let alone its representation precision (RP). Moyer and Landauer (1967) found that the participants reacted faster and more accurately when the magnitude distance between two numbers was larger; this so-called "distance effect" has been extensively replicated in numerical magnitude comparison research. The distance effect

Summary

- Utilizing representational similarity analysis and neural decoding techniques, the research proposes that the fidelity of neural decoding serves as an index of neural representation precision.

- The precision of neural representation of numerical distances in the brain predicts task performance and mathematical arithmetic proficiency in children.

- These findings imply the potential significance of relational information in general cognition and learning beyond mathematical learning.

follows Weber's Law (a principle in psychology that indicates the relationship between the intensity of a stimulus and the minimum amount of change required to detect a difference in that stimulus) (Merten and Nieder 2009; Weber 1948), with reaction time (RT) and accuracy varying as a function of distance/ratio between the numerical sets (Haist et al. 2015). However, the distance effect per se cannot indicate the precision of distance representation, nor can it determine the precision of magnitude representation. On the one hand, a greater distance effect might imply the capacity to detect the different distances between magnitudes, suggesting a clear or possibly accurate magnitude representation. That might explain why the ratio/distance effect increases over development (Haist et al. 2015; Lyons et al. 2015) and correlates positively with arithmetic or mathematics ability (Rousselle and Noel 2007). On the other hand, individuals with more accurate magnitude/distance representation may react quickly even when number sets are close, resulting in a reduced distance effect. This could account for findings of decreasing distance effect during development (Holloway and Ansari 2010; Sekuler and Mierkiewicz 1977) and its correlation with higher numerical acuity and even better math achievement (Ashkenazi et al. 2008, 2009; De Smedt et al. 2009; Mundy and Gilmore 2009). Additionally, inconsistencies in the neuroimaging study—such as conflicting findings of greater activation for the distance effect in the intraparietal sulcus (IPS) in developmental dyscalculia (Ashkenazi et al. 2008) versus lower activation (Mussolin et al. 2010; Price et al. 2007) highlight the complexity of the distance effect.

Generally, symbolic number processing is considered more sensitive to individual differences in math achievement (De Smedt et al. 2013; Matejko and Ansari 2017). In contrast, research on non-symbolic magnitude processing has produced more incongruent findings (see review of Bert De Smedt et al. 2013). This raises doubts about the impact of the approximate number system (ANS) (Cantlon et al. 2009; Feigenson et al. 2004) on mathematics ability. While the paradox of the distance effect persists, the Weber fraction value is widely accepted as a measure of the acuity of magnitude discrimination (Pica et al. 2004). Halberda et al. (2008) further demonstrated that the Weber fraction correlates with math achievement, a finding later replicated by preschool (Libertus et al. 2011) and college students sample (Libertus et al. 2012), further complementing findings across the lifespan (Halberda et al. 2012). They found the number acuity improves throughout school-age

years, peaking at 30 years old. A meta-analysis by Schneider et al. (2017) summarized findings from 45 articles with 17,201 participants and concluded that the Weber fraction correlated more strongly with mathematical achievement than the distance/ratio effect (Also see Chen and Li 2014). However, it remains unclear whether the acuity in magnitude comparison tasks derives from precise distance representation. Moreover, no neural index has yet been established to describe the ability to precisely differentiate two compared stimuli, comparable to the behavioral Weber fraction.

The tuning curve model proposes that magnitudes are represented as neural tuning curves with Gaussian distribution centered on each magnitude. The width of these curves increases linearly with the magnitudes (Lyons et al. 2015; Merten and Nieder 2009; Nieder 2005). Magnitude comparison performance depends on the overlap of these tuning curves, and with narrower curves indicating greater precision. While this model builds on the representation of individual magnitudes, the current study proposes an alternative: individuals may also represent the distance between two magnitudes directly, akin to a "ruler". According to the "three parietal circuits hypothesis" (Dehaene et al. 2003), the core system underlying magnitude and distance representation might rely on a common quantity system. The distinction between these two forms of representations may reflect the difference between encoding a single magnitude and representing the relative relation between two magnitudes. The current study focuses on the effect of these two representations on magnitude comparison task.

Although no brain imaging study to date has directly addressed distance representation in number processing or math learning, research on navigation in physical or cognitive maps suggests that distance representation is crucial for cognition and learning (Theves et al. 2019; Vigano and Piazza 2020). These studies found the involvement of the hippocampus (HIPP) or entorhinal cortex in distance decoding through multivariate voxel pattern analysis (MVPA) and neural representational similarity analysis (RSA). A similar method has been used in numerical-related studies to investigate magnitude representation (Damarla et al. 2016; Eger et al. 2015; Wilkey et al. 2020), primarily focusing on the parietal area, yet no research has specifically addressed the precision of distance representation in numerical contexts. Previous approaches to studying magnitude RP have focused on measures such as functional connectivity or neural pattern similarity. For instance, Zhang et al. (2023) have claimed that the summed functional connectivity within the numerosity network could serve as a biomarker for non-verbal number acuity, but this approach does not directly quantify the degree of acuity. Similarly, Rothlein et al. (2018); Zheng et al. (2018) emphasized neural fidelity in episodic memory and stimulus representation tasks. However, precise representation requires not only stable neural patterns for repeated stimuli, thereby leading to their similarity, but also a clear distinction between different stimuli. Recent work by Barretto-Garcia et al. (2023), using a noisy logarithmic coding (NLC) model (Khaw et al. 2021), linked magnitude neural representation acuity to risk decision. However, this approach falls short when applied to abstract representation like distance, where defining a concrete "receptive field" is inherently

challenging. To date, no study has revealed the neural precision of distance representation in number processing.

Given the limitation of existing approaches, neural decoding offers a novel and promising method to address these gaps. Neural decoding uses machine learning to recognize patterns of neural activity associated with specific features, such as numerical distance/magnitude, and to distinguish responses to different stimuli. This approach enables a direct assessment of neural RP, defined as the fidelity with which neural activity patterns differentiate between stimuli. Decoding fidelity is operationalized as the correlation between the neural decoder's predictions and the actual distances or magnitudes presented in each trial. Importantly, neural decoding surpasses traditional measures by providing a precise and objective way to predict the information of stimulus features, semantic representations, or mental states from the brain activation pattern (Frisby et al. 2023). While prior research has demonstrated the feasibility of decoding numerical magnitude in both nonsymbolic and symbolic forms (Bulthé et al. 2015; Damarla et al. 2016), no study has yet applied this method to investigate distance representation, marking a significant innovation in the current study.

School-aged children were chosen as participants because this developmental period is critical for the refinement of numerical and mathematical skills, providing a unique opportunity to examine the foundational cognitive processes underlying math learning. Additionally, focusing on this age group allows the study to explore how non-symbolic representations driven by the ANS contribute to formal mathematical development. The ANS, which facilitates intuitive and non-symbolic numerical understanding, is considered less influenced by formal education. By using a non-symbolic task, the study seeks to find the potential factors contributing to the incongruent results in prior studies regarding the relationship between the ANS and mathematical ability, providing greater clarity on the role of RP.

The present study aims to address three key objectives: First, to determine whether neural distance representation exists during magnitude comparison tasks using neural decoding methods. Second, to test the effect of distance representation and magnitude representation using the neural tuning curve model (Lyons et al. 2015; Merten and Nieder 2009). Third, to evaluate the precision of distance representation as assessed by neural decoding fidelity and its correlations with task performance and arithmetic performance. By integrating these innovative approaches, the study seeks to advance our understanding of how precise neural representations of distance contribute to mathematical cognition and learning in children.

2 | Materials and Methods

2.1 | Participants

A total of 32 healthy voluntary children were initially recruited for this study. Three participants were excluded due to either incomplete imaging data ($N=1$) or the presence of structural image anomalies ($N=2$). The ART toolbox was employed to detect artifact points with two criteria: (1) frame-to-frame displacement $> 0.5 *$ voxel size; (2) signal amplitude surpassing three standard deviations above the average whole-brain signal. Subjects were eliminated when more than one-third of the time points exhibited artifacts. Ultimately, no subject was eliminated due to measurement artifacts. Consequently, 29 participants (16 males, mean age $= 8.61 \pm 0.92$) were included in the analyses. All participants were right-handed, had normal or corrected-to-normal vision, and had no history of neurological diseases. Written informed consent was obtained from the parents of all child participants, and the children themselves also gave their assent to participate in the study. Ethical approval of the study was granted by the Institutional Review Board of the Institute.

2.2 | Stimuli and Experimental Design

Each participant completed the dot number comparison task in the scanner and the basic arithmetic fluency test outside the scanner.

In the dot comparison task, all stimuli consisted of arrays of black dots presented on a gray circular area against a black background (Figure 1A). The number of dots ranged from 1 to 9. The total area and density were kept constant across all stimuli, while the element size of each dot and its presentation location were randomized. The numerical distance between stimuli ranged from 1 to 6, and the magnitude of the dot pairs and their numerical distances were orthogonalized. So, 12 basic dot pairs were used: 5–6, 4–6, 5–7, 2–5, 3–6, 4–7, 1–5, 4–8, 2–7, 3–8, 2–8, and 3–9. The order in which the two dot patterns within each pair were presented was counterbalanced, resulting in 24 pairs in total. Each pair was repeated three times, yielding a total of 72 trials. These trials were randomly distributed across three runs, each consisting of four mini-blocks of six trials. Four rest blocks were interspersed between the task blocks in each run. The stimuli were presented in a pseudo-random sequence, ensuring that no more than four consecutive trials required the same response side, and the same pair of stimuli was not presented consecutively.

During the fMRI scanning, participants viewed centrally presented dot arrays in succession. Participants were instructed to respond with one of the two buttons depending on whether the first or second number was larger; if the first number was larger, then press the leftmost button with the thumb of the left hand, and if the second number was larger, then press the rightmost one with the thumb of the right hand. The button pressed was balanced across trials. The presentation details for each trial were shown in Figure 1.

2.3 | Weber Fraction Estimation

The Weber fraction estimated each participant's minimum distinguishable difference between the number of dots and which was also known as the ANS (Approximate number system) acuity. The Weber Fraction score was assessed for 29 subjects using the accuracy (ACC) of the dot comparison task. The percentage correct was modeled for each individual subject as 1—error rate (Halberda et al. 2008), where the error rate is defined as:
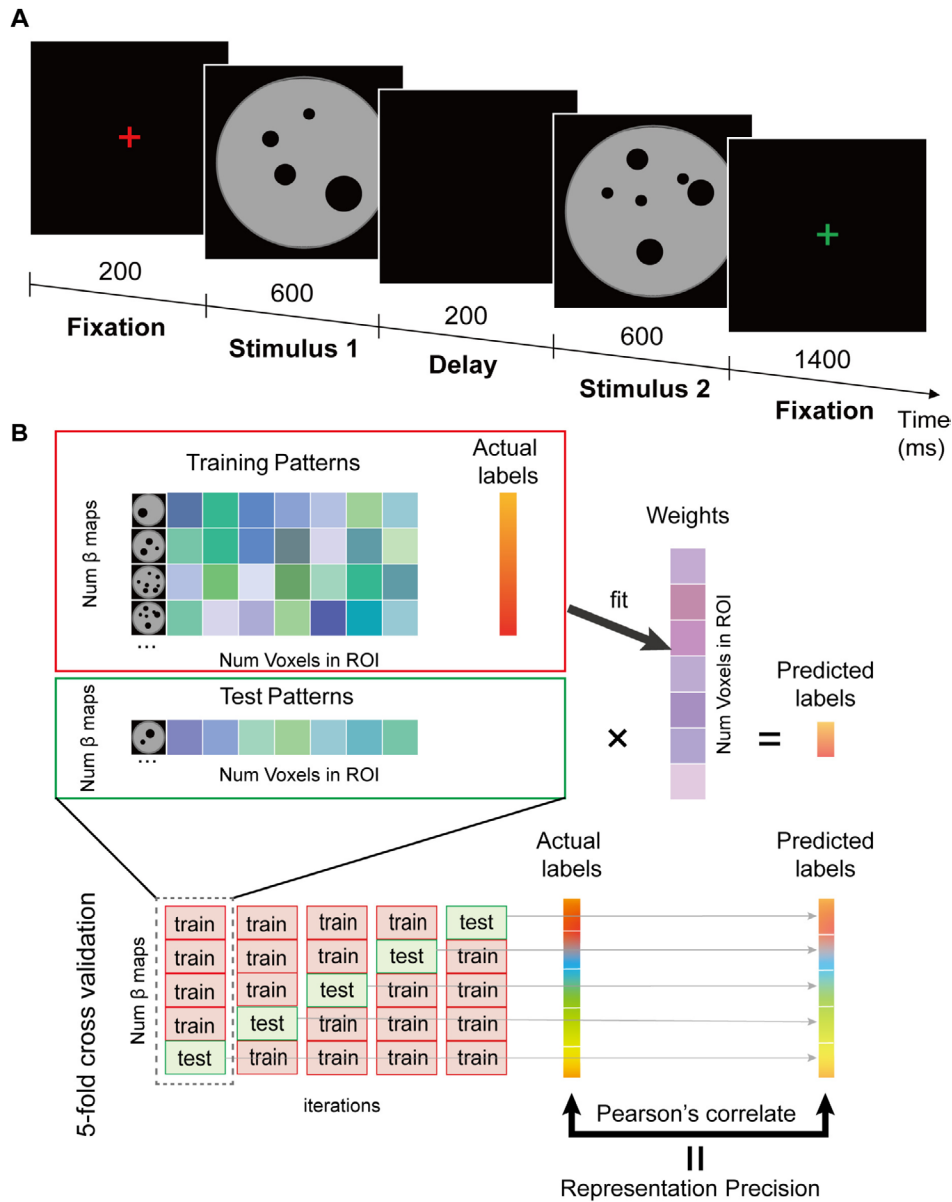
FIGURE 1 | Illustration of the task design and decoding procedure. (A) The illustration of the dot pattern comparison procedure. Subjects needed to compare the two numerical stimuli and decide which one was larger. (B) We first divided the data into a training set with 4/5 trials and a test set with the remaining 1/5 trials. In the training phase, the pattern from 4/5 training trials and their actual labels (distance or magnitude) were used to fit a model (set of weights on each voxel). During the testing phase, the test patterns were multiplied by the weight vector to generate predicted labels (which could take on any real value). A 5-fold cross-validation was conducted which iteratively left out 1/5 trials. Performance was assessed by computing the correlation between the actual and predicted labels (aggregated across iterations).

$$\frac{1}{2} erfc\left(\frac{n_1 - n_2}{\sqrt{2}w\sqrt{n_1^2 + n_2^2}} \right)$$

where $erfc(x)$ is the complementary error function, which is associated with the integral of the normalized Gaussian distribution. This model describes the percentage of correct responses as a function of the Gaussian approximation of number representations for the two dot sets presented in each trial, namely n_1 and n_2 (i.e., n_1 is the numerosity of the larger set, n_2 is the numerosity of the smaller set), with a single adjustable parameter, the Weber fraction (w).

2.4 | Arithmetic Fluency Test

The basic arithmetic fluency test assessed the subject's math performance using timing arithmetic tasks, including addition, subtraction, multiplication and division [adapted from (Wei et al. 2012)]. The Split-half reliability for the arithmetic assessment was 0.98 (calculated based on the dataset of Li et al. (2015)). During the test, a math problem was presented at the center of the screen, with two answer choices displayed below it. For addition and subtraction problems, the deviation of the incorrect answer from the correct one was ±1 or ±2. For multiplication and division, the deviation was ±2 to ensure participants could not rely on clues such as odd or even patterns to identify the correct answer. Participants

press "Q" or "P" to select the correct answer, corresponding to the left or right position respectively. Each arithmetic task was timed at 50 s, resulting in a total test of 200s, with an additional practice section before the formal test. The program recorded the subject's accuracy (ACC) and RT for each problem.

The subject's performance on each type of problem was compared with the dataset of primary school students in the city (Li et al. 2015). The subject's arithmetic performance index (***Z_arithmetic***) was calculated as follows:

$$Z\_arithmetic = (SUM - Ave) / Sd$$

$$SUM = ADD / TIME + SUB / TIME + MUL / TIME + DIV / TIME$$

where, ***ADD***, ***SUB***, ***MUL***, and ***DIV*** are respectively the difference between the number of correct and incorrect problems for each condition. ***TIME*** is the time taken to complete each type of problem. ***Ave*** and ***Sd*** are the average and standard deviation of the group of primary school students for each grade (Table S1).

2.5 | MRI Acquisition Procedure

Images were acquired on a 3.0 T Siemens MRI scanner using a 64-channel head coil. Visual stimuli were projected onto a screen behind the scanner, which was made visible to the participant through a mirror attached to the head coil. Functional images were collected using a single-shot echo-planar imaging (EPI) sequence (axial slices, 33; slice thickness, 3.5 mm; gap, 0.7 mm; TR, 2000 ms; TE, 30 ms; flip angle 90°; voxel size, $3.125 \times 3.125 \times 3.125$ mm³, FOV, 200×200 mm²; volume, 158), while structural images were acquired through three-dimensional sagittal T_1-weighted magnetization-prepared rapid gradient echo (144 slices; slice thickness, 1.33 mm; TR, 2530 ms; TE, 3.39 ms; voxel size, $1.0 \times 1.0 \times 1.33$ mm3, flip angle, 7°; FOV, 256×256 mm).

2.6 | Preprocessing and Modeling of Neuroimaging Data

Task-fMRI data were preprocessed and analyzed for each participant using Statistical Parametric Mapping (SPM12; http://www.fil.ion.ucl.ac.uk/spm). For each participant, the first five volumes (10 s) of each run were discarded for signal equilibrium. The preprocessing of functional images included slice timing correction and head motion correction. Subsequently, T_1-weighted images were co-registered to each participant's functional image, then segmented into gray matter images and spatially normalized into a common stereotactic Montreal Neurological Institute (MNI) space and resampled into 3-mm isotropic voxels.

2.6.1 | Univariate Analysis

Functional data were analyzed using the general linear model (GLM) for first-level analysis. The current study is based on an original mixed block/event-related design (Chawla et al. 1999)

that included three conditions: dot, visual number, and auditory number comparisons. Each condition was presented in each run, consisting of four mini-blocks of six trials, arranged with a Latin square design. Additionally, four rest blocks were interspersed randomly between the task blocks in each run. In the present study, we focus solely on the dot task to start investigating distance representation in basic magnitude processing. To examine the general task-related activation, we set up all three conditions as the regressors that included the block start time and duration. In addition, the Friston 24-parameter model of head motion (Friston-24) was included in the model as additional regressors. This model encompasses 24 movement parameters, which include the 6 standard head motion parameters, the six derivatives of these standard motion parameters, and the 12 corresponding squared terms (Friston et al. 1996; Shirer et al. 2015). A high-pass filter with a cutoff of 1/128 Hz was applied to remove low-frequency drifts. Then, we analyzed the whole-brain data for the dot comparison condition. For group analysis, the brain activation of the dot comparison condition contrast to rest was calculated to obtain the whole-brain activation. The threshold of $p < 0.05$, voxel-level familywise error (FWE) corrected.

To estimate brain activity related to the magnitude size effect and distance effect, we modeled the fMRI data using a GLM with the event-based regressors. There were two events related to distances: close (1–3) and far (4–6). Due to a limitation in the experimental design, while the response hand was counterbalanced for each trial, participants were instructed only to select the larger magnitude. Consequently, the second magnitude values (1–4 and 6–9) are confounded with hand responses. To address this, small and large magnitude events were defined by two subgroups (for 1–4: small:1–3, large: 4; for 6–9: small: 6–7, large: 8–9), followed by a conjunction analysis to integrate the size effect contrast between small and large magnitudes. All events across all conditions were entered as regressors of interest in the GLM. The 24 movement parameters were included as regressors of no interest in the GLMs. Each regressor was convolved with a canonical hemodynamic response function. The model for each participant was high-pass filtered with a cutoff of 1/90 Hz. Group-level analyzes were conducted using SPM12, where t-tests were performed on the resulting contrasts across participants.

2.6.2 | Multivariate Analysis

The normalized, unsmoothed EPI volumes were entered into a GLM to generate beta maps as model input for decoding analysis, with the second stimulus in each trial modeled as a regressor. To ensure that the population neural patterns were not affected by confounding factors such as distraction or random choice, only correct trials were modeled, resulting in an average of 64.8 correct regressors (ranging from 53 to 71) out of 72 total trials, along with a single error regressor (grouping all error trials as a single regressor) for each participant. The onsets of these regressors were convolved with a standard hemodynamic response function. Additionally, 24 regressors of no interest corresponding to the 24 motion parameters, spike regressors detected using the ART toolbox, and a constant regressor for each run were included in the GLM with a high-pass filter with a cut-off frequency of 1/90 Hz. The resulting

beta estimates for the "second number" stimulus conditions were z-scored within each run and then employed in the multi-voxel decoding analysis.

Prior to conducting RSA analysis, the unsmoothed EPI volumes for all 72 trials were entered into the GLM. The second stimulus in each trial was treated as an individual regressor in the GLM. Furthermore, the first stimulus and rest periods were grouped, respectively, and included in the model as two separate regressors of no interest. Twenty-four motion regressors, spike regressors, and a constant regressor for each run were included as nuisance regressors to remove any unwanted variance. A high-pass filter with a cut-off frequency of $1/90\,Hz$ was applied. Subsequently, t maps were derived from each regressor of interest to compute the dissimilarity matrix.

2.7 | ROI Definition

Since the IPS has been extensively reported in numerical cognition and mathematics learning, ranging from basic non-symbolic magnitude perception and symbolic number processing to complex mathematical problem solving (For comprehensive reviews, see Ansari 2008; Arsalidou and Taylor 2011; Brannon 2006; Butterworth et al. 2011; Dehaene et al. 2003; Fias et al. 2013; Menon 2015; Nieder 2004, 2005; Nieder and Dehaene 2009; Peters and De Smedt 2018). Bilateral Intraparietal sulcus (IPS), Left IPS, and Right IPS were selected as regions of interest (ROIs) using the SPM anatomy toolbox (Eickhoff et al. 2005) in the analysis of magnitude and distance representation (Figure 3A).

Additionally, in order to compare the decoding results with a previous distance decoding study, HIPP from the WFU pick-Atlas (Maldjian et al. 2003) was selected as the contrast for the analysis of distance representation, generating Bilateral HIPP, Left HIPP, and Right HIPP as ROIs.

2.8 | Decoding Analysis

Linear support vector regression (SVR) with a regularization parameter $C=1$ was used in scikit-learn (http://scikit-learn.org/stable/) to decode number magnitude or distance of each trial. A 5-fold cross-validation method was utilized. The dataset was randomly divided into five equal parts, with each part serving as the test set once, while the remaining four parts were combined to form the training set. This process was repeated five times, and the decoding performance was evaluated by calculating Pearson's r between target labels and predictions across the entire cross-validation circle (Figure 1B). Notably, for the magnitude decoding, we also split the trials into two sets of "1–4" (also always left-handed response) and "6–9" (right-hand). We then performed decoding within each of these sets separately and combined the predictions to calculate the overall decoding performance. The predictions and original magnitudes within each group were centralized before combining them for performance calculation, ensuring a more conservative correlation. A Fisher-Z transformation was conducted on Pearson's r, defining z_r as the index of representational precision (RP), which measured how precisely

neural population activity represents number distances and magnitudes.

Decoding performance was tested on a group level using one-sample t-tests and permutation tests. In the permutation test, the labels of each trial were shuffled, and 1000 iterations of the entire decoding procedure were performed to obtain the null distribution of decoding performance, and the p value was calculated by the number of times that the decoding performance in the set of 1000 permutation tests outperformed the real decoding performance divided by 1000. P values were corrected for multiple comparisons using FDR (Benjamini and Hochberg 1995).

2.9 | Representational Similarity Analyzes

2.9.1 | Neural Representational Dissimilarity Matrices (RDMs)

The RDMs were calculated using T map for each trial generated from GLM (Misaki et al. 2010). The Dissimilarity between two trials was computed as $1 - r$, where r was calculated using partial Pearson correlation including baseline activity as a covariate. This serves as a statistical means to reduce the influence of elements of no interest, such as shared vascular, neural, and imaging factors, which could lead to high correlations unrelated to the functional elements of interest (Lyons et al. 2015).

2.9.2 | Behavioral Representational Dissimilarity Matrix

For behavioral data, the Euclidean distance of response times (RT) between pairs of trials was computed to generate a trial-by-trial behavioral RDM with dimensions of 72 by 72. Both correct and incorrect trials provide valuable information about the representational structure and the neural patterns underlying task performance. This is because differences in accuracy can serve as indicators of the distance effect. Thus, all trials were included in the RSA analysis to comprehensively capture these effects.

2.9.3 | Computation of Distance and Magnitude Tuning Curve Models

The "Magnitude" model (Figure 2A) used simulated neuronal tuning curves for number magnitude, where the tuning curve is defined as a Gaussian function with widths linearly increasing with number magnitude. The hypothesis posits that the observed neural patterns of similarity relations between pairs of numbers correspond to the degree of overlap predicted by these tuning curves, as validated by Lyons et al. (2015). In the present study, the dissimilarity of magnitude is defined as the 1—overlap (calculated by the proportion of those curves that overlap with one another) of two numbers. By assessing the overlap of curves for any two magnitudes, the magnitude tuning curve overlap matrix was readily obtained (Figure 2A,D). To generate the trial-by-trial magnitude RDMs, referred to as "Magnitude" RDM, the magnitude of the second stimulus in each trial was used as a category label. Each value
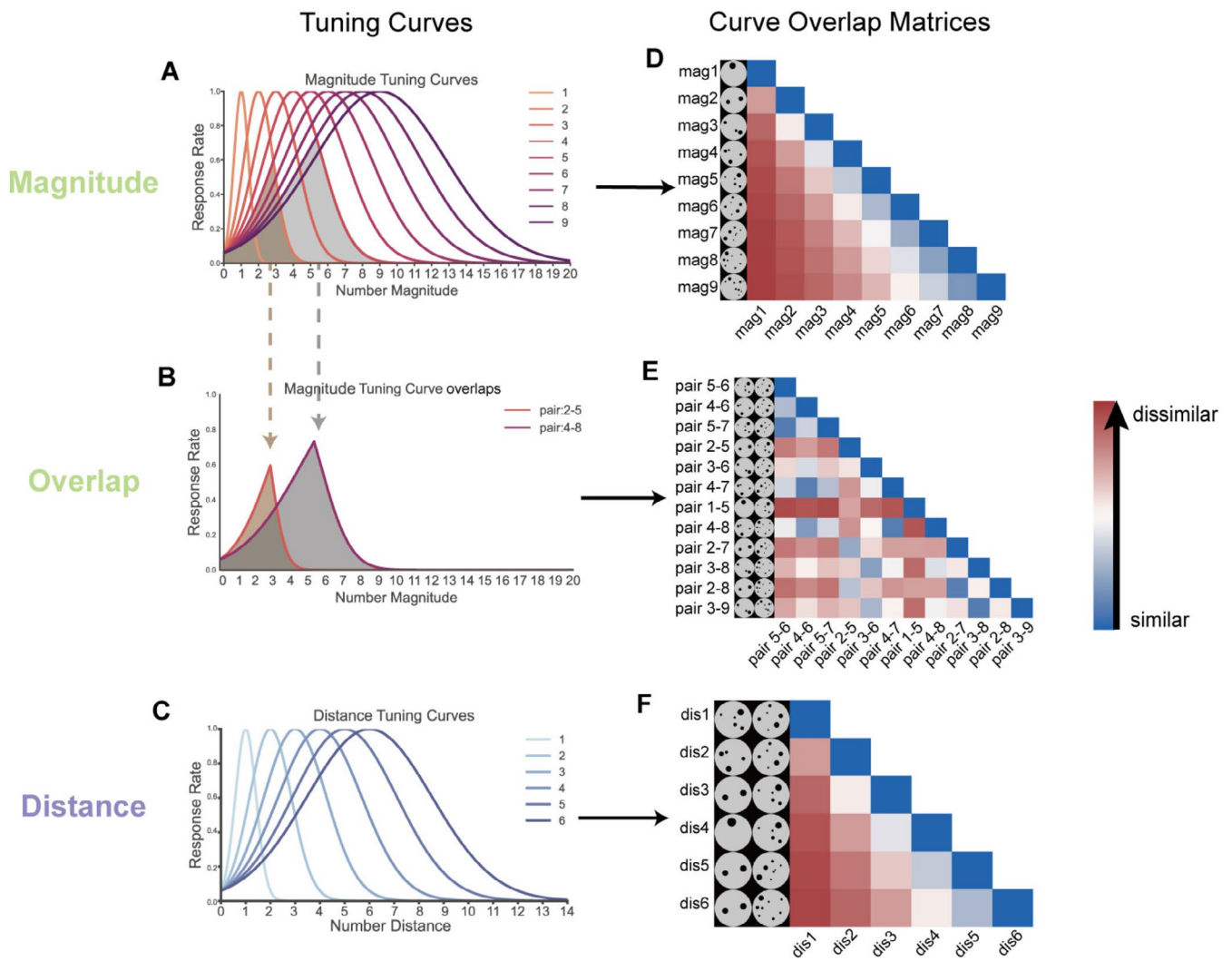
FIGURE 2 | Generating curve overlap matrices simulated neuronal tuning curves for number magnitude (A), distance (C) and overlap curve for magnitude (B); Gaussian functions were computed with width linearly increasing with number magnitude or distance, consistent with human behavioral data. (D–F) For each pair of tuning curves (overlap curves), these show 1—the proportion of those curves that overlap with one another. Note when the overlap increases, the dissimilarity between two curves decreases.

in the RDM was then filled with the overlap value from the curve overlap matrix corresponding to the magnitudes of the respective trials (Figure 4A). This means that the dissimilarity between any two trials is quantified by how much their corresponding magnitude tuning curves overlap.

The "Distance" RDM was constructed based on the hypothesis that distance tuning functions similarly to the magnitude tuning curve (Figure 2C), with the only difference that the x-axis represents the distance label between two numbers (ranging from 1 to 6 in our experiment). For instance, in a trial where the first dot number is two and the second is five, the magnitude label in "magnitude" model for the second stimulus is "5," while the distance label for this trial is "3." To examine this hypothesis, these curves were employed to generate trial-by-trial distance RDMs. Importantly, distance RDMs were utilized in both behavioral and neural RSA.

The "Overlap" RDM (Figure 2B) was utilized in the behavioral RSA analysis. The overlap of pairs of numbers within a single trial was defined as an "overlap curve", representing the trial's

response evoked by those two numeric magnitudes. According to the magnitude overlapping hypothesis, the behavioral performance for each comparison trial is determined by the overlap of the tuning curves of the two compared magnitude, with the similarity between trials determined by the overlap between their respective overlap curves. The across-trial similarity was then computed by measuring the overlap of the overlap curve with other trials, referred to as the "overlap of overlap" (Figure 2B). For instance, the similarity between a trial comparing two and five and a trial comparing four and eight was computed by assessing the overlap of the overlap curves for 2–5 and 4–8 (Figure 2B). In the experiment, which comprised a total of 12 pairs of overlap categories (Figure 2E), trial-by-trial overlap RDM (Figure 4A) were derived, similar to magnitude RDMs. For clarity, here we use the term "similarity," but the actual computation is dissimilarity, consistent with our previous analyzes.

In order to control potential confounding factors, we also constructed two confounding models that characterize low-level visual similarity and response similarity. (1) Visual RDM: To control for the low-level visual similarity effects between dot images, we
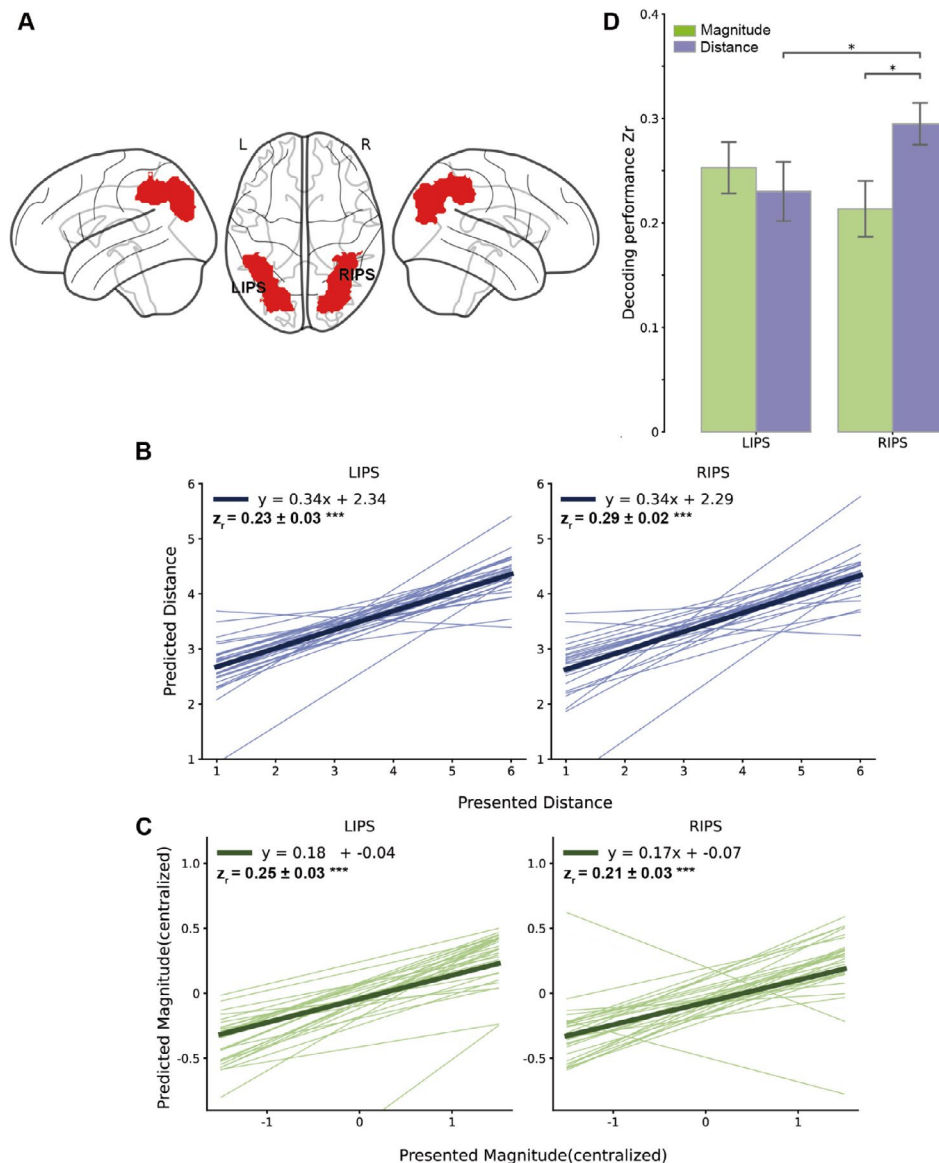
FIGURE 3 | ROIs and SVR decoding results. (A) Regions of interest were defined according to the Julich Brain Atlas. (B, C) The magnitude and distance (the absolute value of the difference between two numbers) were significantly decoded from all three ROIs. Decoding performance was measured using Pearson's correlations between the distance (B) or magnitude (C) of presented number and their predictions obtained using SVR. Each thin line represents an individual subject, the thick line represents the population average. The SVR models were tested in 5-Fold cross validation. z_r was fisher z transformed r and averaged across subject (mean ± s.e.m.). (D) Differences in decoding performance among ROIs. Fisher Z transformed from Pearson's r were averaged across subjects within each region of interest. Error bars reflect s.e.m. (*$p_{corrected} < 0.05$, **$p_{corrected} < 0.01$, ***, $p_{corrected} < 0.001$).

calculated the pixel dissimilarity of image pairs. This dissimilarity was computed by Pearson's correlation distance between the grayscale values of images. (2) Response RDM: A button-press RDM was constructed to control for the effects of motor responses in the dot comparison task. This was computed as the absolute difference between the button press responses (1 for left index finger; 0 for right index finger) recorded during scanning.

2.9.4 | Compare RDMs

The neural RDM and behavioral RDM were then compared with model-based RDMs using Spearman's rank correlation to calculate the "raw effects" of each computation-model RDM. To account for potential confounding factors, partial Spearman's rank correlation was applied, controlling for low-level factors (visual RDM and response RDM) to derive the "preliminary effects" of each computational model RDM. Subsequently, to isolate the "unique effect" of each model, we controlled for other computational models (e.g., controlling for the magnitude model when testing the distance model) during the analysis. The resulting r values were fisher-z transformed for group-level one-sample t-test, assessing whether the RSA results of the theoretical models were significantly greater than zero. Multiple comparisons were corrected using the FDR method (Benjamini and Hochberg 1995).
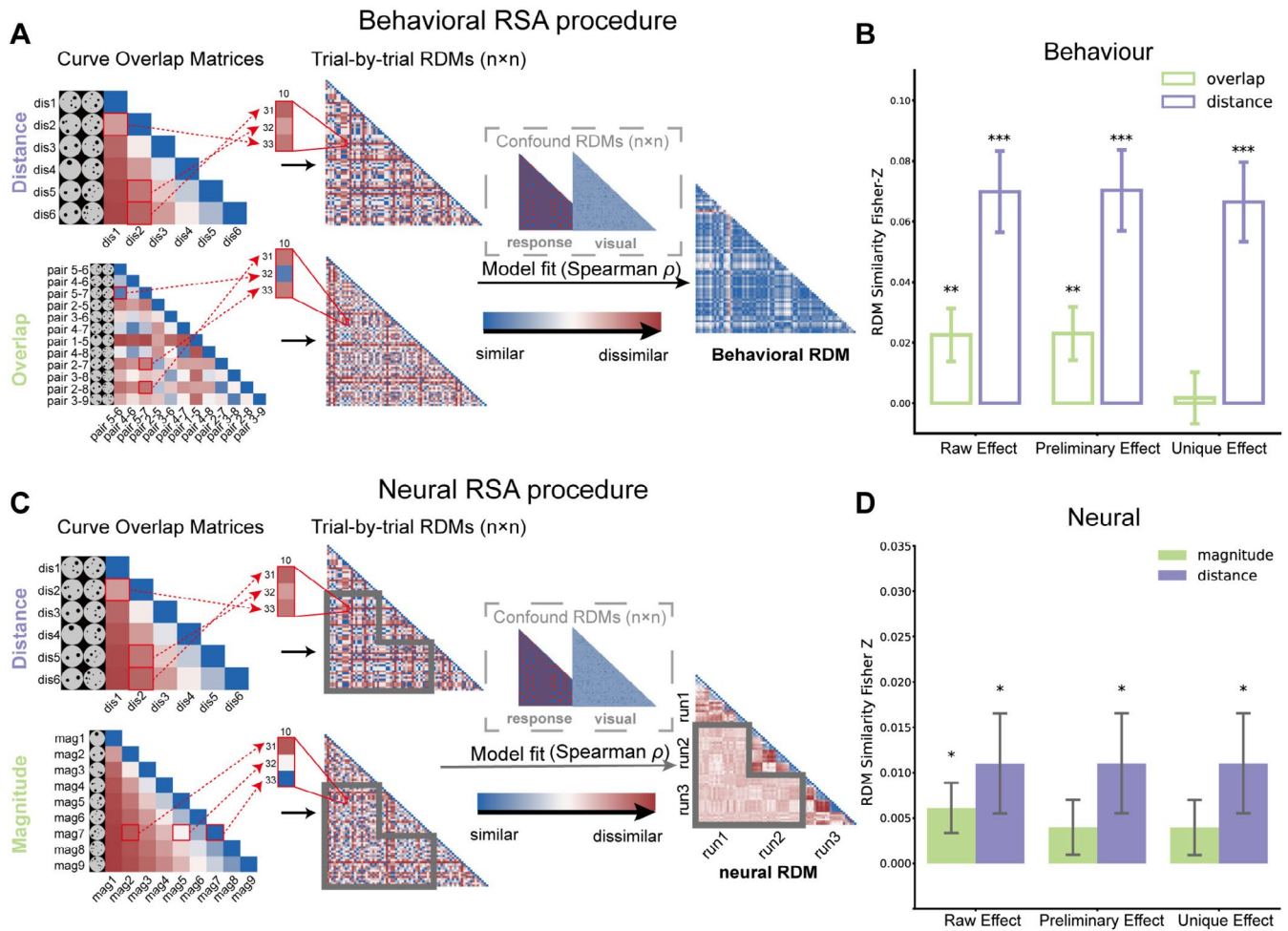
FIGURE 4 | Representational similarity analysis (RSA) procedure and results. This diagram outlines the RSA procedure connecting computational models with brain activity and behavioral data. The left column shows the Curve Overlap Matrices for distances (A top, C top), magnitude (C bottom) and overlap (A bottom) which were generated from tuning curve overlap; The middle column displays trial-by-trial RDMs generated from Curve Overlap Matrices according to each trial's category. The right column exhibits trial-by-trial behavioral RDM, which was defined by the Euclidean distance of RT (A) and the neural RDM (C) calculated by Pearson correlation. Notably, only between-run trials were compared to the neural RDM (indicated with grey frames, (C), while behavior employed full trials. Spearman correlation is employed to associate model RDMs with behavior or neural RDMs. (B) Both the distance and overlap RDMs significantly explain the behavioral differences in reaction times (RT) across trials, but only the distance unique effect is significant. (D) Both the distance RDM and magnitude RDM could significantly explain neural representational geometry in IPS, but only the distance preliminary and unique effects are significant. The bar graph shows the Fisher Z transformed Spearman correlation (partial) coefficient. Group means and standard errors of the similarity are indicated by the bar plots with error bars. The significance of similarity is tested using a one-sample t-test and indicated by a black asterisk: $*p < 0.05$, $**p < 0.01$, $***p < 0.001$, FDR-corrected.

2.10 | Correlation Analysis

The decoding accuracy was correlated with the task and arithmetic performance to reveal the importance of neural RP. Specifically, partial Pearson correlations between Representational Precision (RP, including distance RP and magnitude RP) and math performance were tested. RT and accuracy (ACC) in the dot comparison task were controlled for to ensure that any observed correlation was not attributable to behavioral performance. When testing the correlations between RP and Weber fraction (w), we only controlled for RT, as w was derived from ACC, which could introduce spuriousness or contamination (Becker et al. 2016). The significance level of correlations was also calculated using a permutation test. The label of each trial was shuffled, and 1000 iterations of the whole

decoding procedure and correlation analysis were performed to get the null distribution of partial Pearson correlation r. The p value was calculated by the number of times that the r in the set of 1000 permutation tests outperformed the real r divided by 1000. P values were corrected for multiple comparisons using FDR.

2.11 | Whole Brain Decoding Map and Conjunction Analysis

Trying to get the full picture of brain regions sensitive to distance/magnitude, the SVR decoding models across the whole brain were run, interpreting the model weight of voxels as a decoding map. To select the most important voxels, bootstrap tests

with 1000 samples for each subject were performed (resampling with replacement) (Kohoutová et al. 2022). For every voxel in each individual, uncorrected p values were derived based on the sampling distribution. These p values were obtained by converting z-scores to probabilities using the mean and standard deviation of the sampling distribution. Subsequently, negative logarithmic p values (mean $(-\log(p))$) were computed and voxels corresponding to the top 10% of these mean $(-\log(p))$ values were identified. These selected voxels constituted our predictive map for distance and magnitude.

The binarized predictive map of distance and magnitude was utilized as a mask. By overlaying this mask, a conjunction map was generated. The conjunction map revealed common brain regions that play significant roles in representing both distance and magnitude.

3 | Results

3.1 | Behavioral Results

In the dot comparison task, the average RT was 750 ms (s.d. = 293), and the mean accuracy was 0.90 (s.d. = 0.30). A paired-samples t-test revealed a significant distance effect in both RT ($t = 8.68$, $p < 0.001$) and accuracy ($t = 3.36$, $p < 0.001$). Specifically, RTs for the close distance (796 ms ± 301, (mean ± s.d.)) were slower than for the far distance (704 ms ± 278). Accuracy for the far distance (0.92 ± 0.27) was significantly higher than for the close distance (0.88 ± 0.33). For the magnitude condition, behavioral data could not be extracted for the second stimulus. Thus, the magnitude size effect was evaluated using the sum of the two stimuli (small: 6–9, large: 10–12) (Verguts and Van Opstal 2005). A paired-samples t-test revealed no significant magnitude effect for either RT ($t = -0.40$, $p = 0.691$) or accuracy ($t = -0.52$, $p = 0.606$), replicating previous findings and confirming the insensitivity of the magnitude size effect relative to the distance effect within a certain range of magnitudes (Verguts and Van Opstal 2005).

The arithmetic assessment accuracy was comparatively high, significantly exceeding 50% of the guessing chance (Addition: mean = 0.964, min = 0.800; subtraction: mean = 0.947, min = 0.786; multiplication: mean = 0.968, min = 0.839; division: mean: 0.924, min = 0.667).

3.2 | Univariate Analysis

3.2.1 | Brain Activations Associated With Dot Comparison Task

At the group level, the whole-brain analysis comparing activity during the dot comparison task to rest revealed a network spanning the parietal, occipital, temporal, and frontal lobes (Table S2 and Figure S1), visualized with BrainNet Viewer (version 1.7, Xia et al. 2013; http://www.nitrc.org/projects/bnv/). Notable regions included the bilateral occipital cortex, left middle frontal gyrus, left insular cortex, and right IPS. Additionally, significant negative activation was observed in the left lateral occipital cortex.

3.2.2 | Brain Activations Associated With the Magnitude-Size Effect and Distance Effect

The second univariate analysis involved a voxel-wise t-test to examine which brain areas were significantly modulated by magnitude and distance. The effect of distance was observed in the following brain regions: right inferior temporal gyrus, right postcentral gyrus, right precentral gyrus, left angular gyrus, bilateral IPS, left inferior frontal gyrus, and negative activation in the right insula. The effect of magnitude was observed in the following brain regions: bilateral IPS, bilateral superior frontal gyrus, right frontal pole, and bilateral precentral gyrus. Negative activation was observed in the right middle temporal gyrus and left insula ($p < 0.005$, uncorrected, $k > 100$ voxels) (Table S3 and Figure S2, visualized with BrainNet Viewer (Xia et al. 2013)).

3.3 | Decoding Results of Number Distance and Magnitude

To test whether participants formed a distance representation (the distance between the first and second dot pattern) during the dot magnitude comparison task, SVR was employed to decode number distance. The IPS and the HIPP were chosen as ROI, and fine-grained information was extracted from multivoxel patterns. The distance of each trial was defined as the absolute value of the difference between the first and second dots, treated as continuous variables, and regression was used to detect gradual changes in multivoxel patterns as a function of numerical distance.

The theoretically expected performance in noninformative data corresponds to 0, so the significance level was generated by group level t test against 0. A permutation test was then conducted to further confirm the reliability of these results. The results showed that patterns in IPS were able to predict the number distance (Figure 3B): IPS [($z_r = 0.30 \pm 0.02$ (mean ± s.e.m.)] with 5-fold cross-validation, $p_{\text{perm}} < 0.001$), RIPS ($z_r = 0.29 \pm 0.02$, $p_{\text{perm}} < 0.001$), LIPS ($z_r = 0.23 \pm 0.03$, $p_{\text{perm}} < 0.001$). However, patterns in the HIPP were not able to predict the distance (Figure S4B): HIPP ($z_r = 0.06 \pm 0.02$, $p_{\text{perm}} = 0.099$), RHIPPS ($z_r = 0.05 \pm 0.03$, $p_{\text{perm}} = 0.129$), LHIPPS ($z_r = 0.06 \pm 0.03$, $p_{\text{perm}} = 0.099$). This indicated that the distance information was detected in IPS when subjects performed the number comparison task. RIPS exhibited greater precision in distance decoding compared to LIPS (Figure 3D, paired samples t-test: $t = 2.728$, $p = 0.011$, $p_{\text{corrected}} = 0.039$).

Similar to distance decoding, parallel analysis was conducted to decode number magnitude (the magnitude of the second dot pattern in the comparison task) in IPS ROIs. The decoding results were shown in Figure 3C. Patterns in all ROIs were able to predict the number magnitude: IPS ($z_r = 0.25 \pm 0.02$ (mean ± s.e.m.) with 5-fold cross-validation, $p_{\text{perm}} < 0.001$), RIPS ($z_r = 0.21 \pm 0.03$, $p_{\text{perm}} < 0.001$), LIPS ($z_r = 0.25 \pm 0.03$, $p_{\text{perm}} < 0.001$). The results imply that the subjects access the magnitude representation during the number comparison task as well. There were no differences in magnitude decoding performance between LIPS and RIPS, but we found that distance decoding performance was higher than magnitude in RIPS (Figure 3D, paired samples t-test: RIPS vs. LIPS (mag), $t = 1.376$, $p = 0.180$, $p_{\text{corrected}} = 0.240$;

mag vs. dis (RIPS), $t = 2.476$, $p = 0.020$, $p_{corrected} = 0.039$; mag vs. dis (LIPS), $t = 0.026$, $p = 0.795$, $p_{corrected} = 0.795$). The results of the independent samples t-tests indicated no significant gender differences in the neural representation of both magnitude and distance across IPS ($t_{mag} = 0.803$, $p_{mag} = 0.429$; $t_{dis} = 0.789$, $p_{dis} = 0.437$), LIPS ($t_{mag} = 0.372$, $p_{mag} = 0.713$; $t_{dis} = 0.341$, $p_{dis} = 0.736$), and RIPS ($t_{mag} = 1.431$, $p_{mag} = 0.165$; $t_{dis} = 1.399$, $p_{dis} = 0.174$). Therefore, we did not include gender as a factor in the subsequent analysis.

3.4 | Representational Similarity Analyzes

To provide additional evidence on the effect of distance and magnitude representation on the task, the alignment of the theoretical model of tuning curves overlapping (Lyons et al. 2015) with the observed similarity of neural patterns or behavior, distance, or magnitude was tested.

3.4.1 | Behavioral Patterns of Number Distance and Magnitude Representations

Firstly, it was examined whether the overlapping model of distance or magnitude could account for the behavioral RDM. The trial-by-trial Euclidean distance of RT was used to describe behavioral dissimilarity between trials. The overlap of the tuning curves for the two consecutive numbers within each trial was used to generate a graph representing the magnitude overlap curve (Figure 2A, where the shaded area shows the overlap proportion of the tuning curves for the two consecutive number magnitudes). Each curve reflects the overlap of response elicited by a pair of numbers in a trial, and the overlaps of these curves ("overlap of overlap") indicate the similarities between trials (Figure 2B). So the "overlap" of overlapping tuning curve was then taken as the magnitude overlap to see the relation of it with the dissimilarities of RT between trials (Figure 4A). Note that, the trial-by-trial model RDM was calculated by 1-overlap. Simultaneously, a distance model was applied to establish tuning curves representing the distance between the two numbers within each trial, and the overlap of these distance tuning curves (referred to as "distance overlap") was used to describe trial-to-trial similarity (Figure 2C, Figure 4A).

Results indicated that both models, to some extent, captured behavioral RT geometry (Raw effect: overlap: $z = 0.023$, $p = 0.010$; distance: $z = 0.070$, $p < 0.001$; Preliminary effect: overlap: $z = 0.023$, $p = 0.010$; distance: $z = 0.070$, $p < 0.001$, Figure 4B). However, when mutually controlling for each other, only the unique effect of the distance model remained significant (Unique effect: overlap: $z = 0.002$, $p = 0.42$; distance: $z = 0.066$, $p < 0.001$). This result suggests that the representation of distance between presented numbers within a trial plays a crucial role in explaining behavioral similarity rather than the overlaps of magnitude tuning curves.

3.4.2 | Neural Patterns of Number Distance and Magnitude Representations

It was assumed that the correlation between the distributed patterns of activity for two trials is indeed predicted by the extent to which their tuning curves overlap. Consequently, two types of trial-by-trial RDMs for magnitude and distance were defined based on tuning curve overlap model. To examine the magnitude representation, magnitude RDM was defined to reflect the overlap of the tuning curves for the second number of each trial (referred to as "magnitude of number 2 overlap"). Concurrently, the same RDM for distance representation as employed in our behavioral RSA analysis was used. These RDMs were correlated with neural RDM (Figure 4C), and this correlation was calculated using only across-run trial pairs to control for Type I error (Mumford et al. 2014). Initially, Spearman correlation was used to test the raw effect. Then, visual and response RDMs were included as confound RDMs, and partial Spearman correlation was calculated to test the preliminary effect. Subsequently, the unique effect was introduced by adding the other computational model as a confound RDM.

The results in IPS replicated the findings from Lyons et al. (2015) for magnitude representation. Additionally, the overlaps of distance tuning curves exhibited a similar pattern (Raw effect: magnitude: $z = 0.006$, $p = 0.042$; distance: $z = 0.011$, $p = 0.042$). These indicated that both magnitude and distance models capture neural similarity to some extent. However, after controlling for visual and response RDMs, the significance of the magnitude model diminished, while the distance model significantly correlated with neural similarity (Figure 4D, Preliminary effect: magnitude: $z = 0.004$, $p = 0.101$, distance: $z = 0.011$, $p = 0.042$; Unique effect: magnitude: $z = 0.004$, $p = 0.101$; distance: $z = 0.011$, $p = 0.042$. Table S4).

The results in the HIPP indicated that distance models cannot capture neural similarity in the HIPP (Raw effect: BHIPP: $z = 0.006$, $p = 0.234$, LHIPP: $z = 0.007$, $p = 0.159$; RHIPP: $z = 0.003$, $p = 0.312$, Figure S4C).

3.5 | Neural Distance Representation Precision Related to Individual Differences in Numerical Acuity and Math Performance

After confirming the existence of distance representation through both decoding and RSA analyses, the aim was to define a neural index that describes the precision of representation during a number comparison task. Notably, a higher z_r, between the SVR decoder's prediction and the presented one for a participant indicated that the neural patterns in the IPS represented distance more accurately. Thus, z_r was defined as each individual's RP. It was assumed that individuals would demonstrate greater numerical acuity and better math performance when they have more accurate distance representation.

Consistent with the hypothesis, it was found that distance RP was negatively correlated with the Weber Fraction score (Table 1), which was assessed by psychophysical modeling of performance on the number comparison task. A higher Weber fraction score corresponds to poorer ANS acuity. Correlation: IPS ($r = -0.415$, $p_{perm} = 0.028$). The partial correlation results are shown in Figure 5A: IPS ($r = -0.418$, $p_{perm} = 0.030$). This indicates that individuals with higher neural representation precision of distance have better ANS acuity.

The correlations between the participants' distance RP and their symbolic arithmetic performance were then examined (Table 1).

Positive correlations were observed between RP and arithmetic performance in IPS ($r = 0.501$, $p_{perm} = 0.004$), even after controlling for RT and accuracy of the dot comparison task: IPS (partial $r = 0.384$, $p_{perm} = 0.025$, Figure 5B). These results suggest that individuals who can represent distance more precisely tend to perform better in symbolic arithmetic task.

The correlations between the magnitude RP of the participants and their Weber fraction and symbolic arithmetic performance were also tested. No correlation was found between magnitude RP and the Weber Fraction score. The negative correlations between RP and arithmetic performance in IPS were only marginally significant ($r = -0.343$, $p_{perm} = 0.084$), but when RT and accuracy were taken into account, this association was no longer significant (IPS: $r = -0.320$, $p_{perm} = 0.149$, Figure S3, Table S5).

3.6 | Whole Brain Maps for Distance or Magnitude Decoding

To further detect distance-sensitive brain regions other than IPS, the SVR models were applied to each participant's whole-brain multivoxel pattern, creating 29 individualized distance-decoding maps. Important features for distance decoding were identified using bootstrap tests with 1000 iterations for each individual's map. With the p values from bootstrap tests, the mean $(-\log(p))$ values were computed for the whole brain across all individualized maps, and the top 10% voxels were selected, with a threshold of mean $(-\log(p)) = 1.649$. The selected voxels are displayed in Figure S5A and Table S6. The distance-sensitive map involved widespread regions in the cortex, including the visual cortex, IPS, angular gyrus, precuneus, motor cortex, prefrontal cortex, insula, medial temporal gyrus, and cingulate cortex. The same procedure was applied to find important magnitude-sensitive brain regions, selecting the top 10% voxels, with the threshold being the mean $(-\log(p)) = 1.827$. The selected voxels are displayed in Figure S5B and Table S6. The magnitude predictive map involved widespread regions in the cortex.

Furthermore, a conjunction analysis was performed to identify the common region of the two predictive maps. The results showed that neural signals in the bilateral IPS, left temporal-occipital area, and lingual gyrus play an important role in representing both magnitude and distance (Table S6, and Figure S5C, visualized with BrainNet Viewer (Xia et al. 2013)).

4 | Discussion

Generally, the present study highlights the critical role of distance representation in numerical cognition and its implications for children's mathematical abilities. By employing advanced neural decoding techniques, the study demonstrated that distance information could be accurately decoded from multivoxel patterns in IPS during magnitude comparison tasks. Crucially, the precision of distance presentation—measured through decoding fidelity—was significantly associated with both the Weber fraction and arithmetic performance. These findings emphasize the importance of precise neural distance representations in supporting mathematical cognition, offering fresh insights into the mechanisms underlying numerical processing and learning.

TABLE 1 | Distance RP partial correlations with arithmetic performance and Weber fraction.

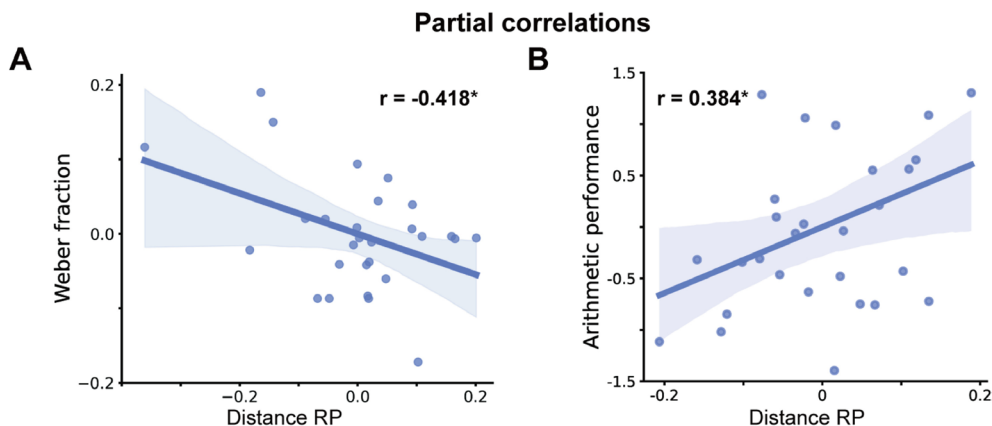|	Correlation		Partial correlation	
	Pearson's r	p-corrected	Pearson's r	p-corrected
Arithmetic	0.501	0.004	0.384	0.025
Weber fraction	−0.415	0.032	−0.418	0.032

FIGURE 5 | Partial correlations. The SVR decoding performance of distance Z_r for each subject was defined as representation precision (RP). (A) Distance RP (decoding performance Z_r) in the IPS was significantly correlated with the Weber fraction (estimated in number comparison task, with lower value indicating better performance) even after controlling for RT. (B) Distance RP also showed a significant association with arithmetic performance after controlling for the RT and accuracy of dot comparison task. Significance of partial correlation is indicated by black asterisk: *$p < 0.05$, p value was generated from permutation test, FDR-corrected.

The study successfully decoded distance information from the IPS, demonstrating that this region encodes not only magnitude (Damarla et al. 2016; Eger et al. 2015) but also the relational differences between numerical values. These findings support the hypothesis that distance representation is a distinct and critical component of numerical cognition. By employing advanced neural decoding techniques, we provide direct evidence that the brain processes relational information, which complements previous findings on magnitude representation. The ability to decode distance representation underscores its centrality in tasks requiring numerical comparison and further supports the notion of a "mental ruler" mechanism for relational judgments.

The RSA results confirm the presence of distance representation during magnitude comparison and further highlight the significance of distance representation over magnitude representation. This builds on prior work by Lyons et al. (2015) who proposed a tuning curve model for magnitude representation. We hypothesized that both magnitude and distance representations share a similar Gaussian-based tuning curve structure in the IPS. This similarity was evidenced by the alignment of the theoretical tuning curve models with both behavioral and neural RDMs (see Figure 4.). Specifically, RSA results confirm that the neural geometry of both magnitude and distance representations reflects Gaussian distributions, which underscores a shared quantity-based representational mechanism in the IPS (Dehaene et al. 2003; Núñez-Peña and Suárez-Pellicioni 2014; Park et al. 2021). Importantly, when mutually controlling for each other, only the distance model survived. Furthermore, the distance model continued to explain the neural RDM even when controlling for visual and response RDMs, whereas the magnitude model could not, suggesting that distance representation plays a dominant role in supporting task performance. This finding builds on earlier work suggesting that the IPS plays a central role in relative numerical judgments (Ansari et al. 2006; Holloway and Ansari 2009; Pinel et al. 2001) and extends it by demonstrating that distance representation is a critical factor in mathematical cognition. Notably, although both distance and magnitude were decoded in bilateral IPS, distance decoding outperformed magnitude decoding in the right IPS. At first glance, this appears to contradict the claim that the left IPS is more involved in precise number representation (Ansari 2007; Vogel et al. 2015). Nonetheless, assuming that the right IPS represents abstract magnitude (Chochon et al. 1999; Cohen Kadosh et al. 2007; Piazza et al. 2007), it is conceivable that the abstract relative information of distance relies more heavily on the right IPS compared to the more concrete magnitude representation (However, the contradictory findings from the whole-brain analysis warrant a cautious interpretation of this result).

Distance representation integrates the relational information between stimuli, forming a foundational element of cognition (Hafri and Firestone 2021; Penn et al. 2008). Previous studies on cognitive maps have established that distance can be encoded. However, the implicated brain regions are predominantly reported as the HIPP or entorhinal cortex rather than the parietal or IPS. One possible explanation is that the subcortical HIPP plays a central role during the initial stages of map construction, with the cortical parietal cortex assisting in later stages as the representation matures, which aligns with the hypothesis of a complementary learning system (McClelland et al. 1995).

This hypothesis is supported by evidence suggesting that extended training regime can lead to the absence of detectable distance-modulated response in the hippocamps (Vigano and Piazza 2020). A second explanation is task specificity: the parietal cortex maybe more engaged when tasks require explicit detection or computation of distances between items. Where many studies on cognitive map did not employ task emphasizing comparative judgments (Vigano and Piazza 2020), which may account for the limited identification of parietal involvement in such process. Additionally, sensitivity to one-dimensional versus multidimensional spaces may vary across brain regions. The parietal cortex's omission as a region of interest in cognitive space studies further complicates the understanding of its role. Those hypotheses warrant further investigation.

Notably, both univariate and whole brain multivariate analyses reveal a network of brain regions involved in distance and magnitude representation beyond the IPS. These findings suggest a broader neural network perspective for future studies. Additional regions, such as the entorhinal cortex (EHC), prefrontal cortex (PFC)—including the dorsolateral (dlPFC) and ventromedial (vmPFC) subdivisions—insula, and anterior temporal lobes, also appear to support distance representation and cognitive map coding. These regions facilitate processes like navigation, semantic relational processing, relational integration, and valuation (Constantinescu et al. 2016; Kriegeskorte and Kievit 2013). Understanding how the IPS interacts with these areas and how the brain organizes semantic and conceptual maps based on the distance representation is worth further investigation.

One of the most significant contributions of this study is the introduction of neural representation precision as a measurable index of distance representation accuracy. The study demonstrates, for the first time, that the precision of distance representation, as indexed by decoding fidelity in the IPS, is strongly predictive of both number acuity and arithmetic performance, while magnitude representation does not. The lack of correlation between magnitude decoding and both task performance and mathematical achievement replicated the null findings reported in the study by Wilkey et al. (2020). These findings extend previous behavioral findings (Cantlon et al. 2009; Halberda et al. 2008; Libertus et al. 2011) by providing a neural basis for the relationship between distance representation and mathematical ability. Moreover, the finding may help resolve inconsistencies in the literature regarding the relationship between numerical magnitude processing and math achievement (see the meta-analysis of Schneider et al. 2017). Specifically, the current study clarifies these discrepancies by demonstrating that distance representation—the ability to perceive and represent the relative difference between two magnitudes—accounts for mathematical proficiency more strongly than magnitude representation alone. This reinforces the idea that mathematical performance hinges more on understanding relationships between numbers than on the absolute magnitude of individual numbers.

Distance representation enables individuals to discern the relative relation between numbers, which is essential for performing arithmetic operations such as addition (e.g., knowing that $2 + 6$ is the same as moving a distance of 6 units from 2) and subtraction (e.g., recognizing how far 9 is from 5). We propose

that detecting relative information based on distance—through identifying, integrating, and manipulating relationships between entities or concepts—is integral to mathematical abstraction. Consequently, manipulating magnitudes, numbers, and mathematical elements likely enhances mathematical learning. This insight aligns with findings by Park et al. (2016); Park and Brannon (2014), who showed that approximate arithmetic training is more effective in improving arithmetic performance than magnitude comparison training. These findings highlight the importance of fostering relational and distance-based processing to support mathematical achievement.

Mathematical reasoning often requires the recognition of patterns, hierarchical structures, and interdependencies that transcend specific instances, which is also central to human cognition. So the importance of relational information extends beyond numerical cognition. Studies in semantic spaces have shown that distance encoding supports relational processing in various domains, including word (Vigano and Piazza 2020; Viganò et al. 2021), concept (Theves et al. 2019) and decision making (Barretto-Garcia et al. 2023; Peters et al. 2008). Recent reviews, such as those by Hafri and Firestone (2021); Halford et al. (2010); Penn et al. (2008), underscore the importance of relational processing in tasks involving comparisons, hierarchical structuring, and problem-solving. This suggests that distance representation may serve as a domain-general factor for relational reasoning, potentially providing a foundation for higher-order cognitive processes.

Future research should explore the role of distance representation across different domains and age groups. While this study focused on school-age children—an important developmental period for mathematical learning—the findings may have broader implications for adults, particularly in contexts requiring relational reasoning and abstraction. Unlike the findings of Haist et al. (2015), which observed a correlation between the neural ratio effect in IPS and math achievement only in children, we hypothesize that the precise neural distance decoding would also be evident in other age groups. Supporting this idea, Halberda et al. (2012) found a consistent increase in number acuity expanding from childhood until adulthood. Additionally, Park and Brannon (2013) demonstrated that approximate arithmetic training can improve arithmetic performance even in adults. Given the different brain networks related to number cognition and arithmetic strategies (Ansari 2008; Ansari and Dhital 2006; Haist et al. 2015; Qin et al. 2014), future studies should compare children, adolescents, and adults, as well as investigate this process across the lifespan. Such research could provide a comprehensive understanding of the neural mechanisms of numerical cognition and relational reasoning, thereby overcoming the current study's limitation of focusing solely on a developmental sample. Furthermore, the modest sample size limits the generalizability of the findings, particularly regarding individual differences in cognitive development. Future studies should include larger and more diverse samples to validate these results.

Generally, the current study first highlights the critical role of distance representation in numerical cognition, demonstrating its dominance over magnitude representation in predicting both task performance and arithmetic proficiency. By introducing neural representation precision as a novel marker, the findings provide a significant advance in our understanding of the neural mechanisms underlying mathematical cognition. Future research should further explore the cognitive components and mechanisms underlying the distance representation, using meticulous and well-controlled designs across different modalities and domains. Exploring these areas will provide deeper insights into the cognitive and neural foundations of relational processing, potentially informing strategies to enhance mathematical and cognitive abilities across various domains, advancing our understanding of cognitive processing and learning.

Conflicts of Interest

The authors declare no conflicts of interest.

Data Availability Statement

The data that support the findings of this study are openly available in github at https://github.com/qwhying/NRPD-predict-arithmetic/tree/main.

References

Ansari, D. 2007. "Does the Parietal Cortex Distinguish Between "10," "Ten," and Ten Dots?" *Neuron* 53, no. 2: 165–167. https://doi.org/10.1016/j.neuron.2007.01.001.

Ansari, D. 2008. "Effects of Development and Enculturation on Number Representation in the Brain." *Nature Reviews Neuroscience* 9, no. 4: 278–291. https://doi.org/10.1038/nrn2334.

Ansari, D., and B. Dhital. 2006. "Age-Related Changes in the Activation of the Intraparietal Sulcus During Nonsymbolic Magnitude Processing: An Event-Related Functional Magnetic Resonance Imaging Study." *Journal of Cognitive Neuroscience* 18, no. 11: 1820–1828. https://doi.org/10.1162/jocn.2006.18.11.1820.

Ansari, D., B. Dhital, and S. C. Siong. 2006. "Parametric Effects of Numerical Distance on the Intraparietal Sulcus During Passive Viewing of Rapid Numerosity Changes." *Brain Research* 1067, no. 1: 181–188. https://doi.org/10.1016/j.brainres.2005.10.083.

Arsalidou, M., and M. J. Taylor. 2011. "Is 2 + 2 = 4? Meta-Analyses of Brain Areas Needed for Numbers and Calculations." *NeuroImage* 54, no. 3: 2382–2393. https://doi.org/10.1016/j.neuroimage.2010.10.009.

Ashkenazi, S., A. Henik, G. Ifergane, and I. Shelef. 2008. "Basic Numerical Processing in Left Intraparietal Sulcus (IPS) Acalculia." *Cortex* 44, no. 4: 439–448. https://doi.org/10.1016/j.cortex.2007.08.008.

Ashkenazi, S., N. Mark-Zigdon, and A. Henik. 2009. "Numerical Distance Effect in Developmental Dyscalculia." *Cognitive Development* 24, no. 4: 387–400. https://doi.org/10.1016/j.cogdev.2009.09.006.

Barretto-Garcia, M., G. de Hollander, M. Grueschow, R. Polania, M. Woodford, and C. C. Ruff. 2023. "Individual Risk Attitudes Arise From Noise in Neurocognitive Magnitude Representations." *Nature Human Behaviour* 7: 1551–1567. https://doi.org/10.1038/s41562-023-01643-4.

Becker, T. E., G. Atinc, J. A. Breaugh, K. D. Carlson, J. R. Edwards, and P. E. Spector. 2016. "Statistical Control in Correlational Studies: 10 Essential Recommendations for Organizational Researchers." *Journal of Organizational Behavior* 37, no. 2: 157–167. https://doi.org/10.1002/job.2053.

Benjamini, Y., and Y. Hochberg. 1995. "Controlling the False Discovery Rate: A Practical and Powerful Approach to Multiple Testing." *Journal of the Royal Statistical Society: Series B: Methodological* 57, no. 1: 289–300. https://doi.org/10.1111/j.2517-6161.1995.tb02031.x.

Brannon, E. M. 2006. "The Representation of Numerical Magnitude." *Current Opinion in Neurobiology* 16, no. 2: 222–229. https://doi.org/10.1016/j.conb.2006.03.002.

Bulthé, J., B. De Smedt, and H. P. Op de Beeck. 2015. "Visual Number Beats Abstract Numerical Magnitude: Format-Dependent Representation of Arabic Digits and Dot Patterns in Human Parietal Cortex." *Journal of Cognitive Neuroscience* 27, no. 7: 1–12. https://doi.org/10.1162/jocn_a_00787.

Butterworth, B., S. Varma, and D. Laurillard. 2011. "Dyscalculia: From Brain to Education." *Science* 332, no. 6033: 1049–1053. https://doi.org/10.1126/science.1201536.

Cantlon, J. F., M. L. Platt, and E. M. Brannon. 2009. "Beyond the Number Domain." *Trends in Cognitive Sciences* 13, no. 2: 83–91. https://doi.org/10.1016/j.tics.2008.11.007.

Chawla, D., G. Rees, and K. J. Friston. 1999. "The Physiological Basis of Attentional Modulation in Extrastriate Visual Areas." *Nature Neuroscience* 2, no. 7: 671–676. https://doi.org/10.1038/10230.

Chen, Q., and J. Li. 2014. "Association Between Individual Differences in Non-Symbolic Number Acuity and Math Performance: A Meta-Analysis." *Acta Psychologica* 148: 163–172. https://doi.org/10.1016/j.actpsy.2014.01.016.

Chochon, F., L. Cohen, P. Van De Moortele, and S. Dehaene. 1999. "Differential Contributions of the Left and Right Inferior Parietal Lobules to Number Processing." *Journal of Cognitive Neuroscience* 11, no. 6: 617–630. https://doi.org/10.1162/089892999563689.

Cohen Kadosh, R., K. Cohen Kadosh, A. Kaas, A. Henik, and R. Goebel. 2007. "Notation-Dependent and Independent Representations of Numbers in the Parietal Lobes." *Neuron* 53, no. 2: 307–314. https://doi.org/10.1016/j.neuron.2006.12.025.

Constantinescu, A. O., J. X. O'Reilly, and T. E. J. Behrens. 2016. "Organizing Conceptual Knowledge in Humans With a Gridlike Code." *Science* 352, no. 6292: 1464–1468. https://doi.org/10.1126/science.aaf0941 %J Science.

Damarla, S. R., V. L. Cherkassky, and M. A. Just. 2016. "Modality-Independent Representations of Small Quantities Based on Brain Activation Patterns." *Human Brain Mapping* 37, no. 4: 1296–1307. https://doi.org/10.1002/hbm.23102.

De Smedt, B., L. Verschaffel, and P. Ghesquiere. 2009. "The Predictive Value of Numerical Magnitude Comparison for Individual Differences in Mathematics Achievement." *Journal of Experimental Child Psychology* 103, no. 4: 469–479. https://doi.org/10.1016/j.jecp.2009.01.010.

De Smedt, B., M.-P. Noël, C. Gilmore, and D. Ansari. 2013. "How Do Symbolic and Non-Symbolic Numerical Magnitude Processing Skills Relate to Individual Differences in Children's Mathematical Skills? A Review of Evidence From Brain and Behavior." *Trends in Neuroscience and Education* 2, no. 2: 48–55.

Dehaene, S. 1992. "Varieties of Numerical Abilities." *Cognition* 44, no. 1–2: 1–42. https://doi.org/10.1016/0010-0277(92)90049-n.

Dehaene, S., M. Piazza, P. Pinel, and L. Cohen. 2003. "Three Parietal Circuits for Number Processing." *Cognitive Neuropsychology* 20, no. 3–6: 487–506. https://doi.org/10.1080/02643290244000239.

Eger, E., P. Pinel, S. Dehaene, and A. Kleinschmidt. 2015. "Spatially Invariant Coding of Numerical Information in Functionally Defined Subregions of Human Parietal Cortex." *Cerebral Cortex* 25, no. 5: 1319–1329. https://doi.org/10.1093/cercor/bht323.

Eickhoff, S. B., K. E. Stephan, H. Mohlberg, et al. 2005. "A New SPM Toolbox for Combining Probabilistic Cytoarchitectonic Maps and Functional Imaging Data." *NeuroImage* 25, no. 4: 1325–1335. https://doi.org/10.1016/j.neuroimage.2004.12.034.

Feigenson, L., S. Dehaene, and E. Spelke. 2004. "Core Systems of Number." *Trends in Cognitive Sciences* 8, no. 7: 307–314.

Fias, W., V. Menon, and D. Szucs. 2013. "Multiple Components of Developmental Dyscalculia." *Trends in Neuroscience and Education* 2, no. 2: 43–47. https://doi.org/10.1016/j.tine.2013.06.006.

Frisby, S. L., A. D. Halai, C. R. Cox, M. A. Lambon Ralph, and T. T. Rogers. 2023. "Decoding Semantic Representations in Mind and Brain." *Trends in Cognitive Sciences* 27, no. 3: 258–281. https://doi.org/10.1016/j.tics.2022.12.006.

Friston, K. J., S. Williams, R. Howard, R. S. Frackowiak, and R. Turner. 1996. "Movement-Related Effects in fMRI Time-Series." *Magnetic Resonance in Medicine* 35, no. 3: 346–355. https://doi.org/10.1002/mrm.1910350312.

Hafri, A., and C. Firestone. 2021. "The Perception of Relations." *Trends in Cognitive Sciences* 25, no. 6: 475–492. https://doi.org/10.1016/j.tics.2021.01.006.

Haist, F., J. H. Wazny, E. Toomarian, and M. Adamo. 2015. "Development of Brain Systems for Nonsymbolic Numerosity and the Relationship to Formal Math Academic Achievement." *Human Brain Mapping* 36, no. 2: 804–826. https://doi.org/10.1002/hbm.22666.

Halberda, J., M. M. M. Mazzocco, and L. Feigenson. 2008. "Individual Differences in Non-Verbal Number Acuity Correlate With Maths Achievement." *Nature* 455, no. 7213: 665–668. https://doi.org/10.1038/nature07246.

Halberda, J., R. Ly, J. B. Wilmer, D. Q. Naiman, and L. Germine. 2012. "Number Sense Across the Lifespan as Revealed by a Massive Internet-Based Sample." *Proceedings of the National Academy of Sciences* 109, no. 28: 11116–11120. https://doi.org/10.1073/pnas.1200196109.

Halford, G. S., W. H. Wilson, and S. Phillips. 2010. "Relational Knowledge: The Foundation of Higher Cognition." *Trends in Cognitive Sciences* 14, no. 11: 497–505. https://doi.org/10.1016/j.tics.2010.08.005.

Holloway, I. D., and D. Ansari. 2009. "Mapping Numerical Magnitudes Onto Symbols: The Numerical Distance Effect and Individual Differences in Children's Mathematics Achievement." *Journal of Experimental Child Psychology* 103, no. 1: 17–29. https://doi.org/10.1016/j.jecp.2008.04.001.

Holloway, I. D., and D. Ansari. 2010. "Developmental Specialization in the Right Intraparietal Sulcus for the Abstract Representation of Numerical Magnitude." *Journal of Cognitive Neuroscience* 22, no. 11: 2627–2637. https://doi.org/10.1162/jocn.2009.21399.

Khaw, M. W., Z. Li, and M. Woodford. 2021. "Cognitive Imprecision and Small-Stakes Risk Aversion." *Review of Economic Studies* 88, no. 4: 1979–2013. https://doi.org/10.1093/restud/rdaa044.

Kohoutová, L., L. Y. Atlas, C. Büchel, et al. 2022. "Individual Variability in Brain Representations of Pain." *Nature Neuroscience* 25, no. 6: 749–759. https://doi.org/10.1038/s41593-022-01081-x.

Kriegeskorte, N., and R. A. Kievit. 2013. "Representational Geometry: Integrating Cognition, Computation, and the Brain." *Trends in*

Cognitive Sciences 17, no. 8: 401–412. https://doi.org/10.1016/j.tics.2013.06.007.

Li, X., J. Yang, H. Lu, F. Wang, and H. Zhao. 2015. "The Basic Numerical Magnitude Processing Deficit and Cognitive Characteristics of Developmental Dyscalculia." *Chinese Jounral of Special Education* 182, no. 8: 56–63.

Libertus, M. E., D. Odic, and J. Halberda. 2012. "Intuitive Sense of Number Correlates With Math Scores on College-Entrance Examination." *Acta Psychologica* 141, no. 3: 373–379. https://doi.org/10.1016/j.actpsy.2012.09.009.

Libertus, M. E., L. Feigenson, and J. Halberda. 2011. "Preschool Acuity of the Approximate Number System Correlates With School Math Ability." *Developmental Science* 14, no. 6: 1292–1300. https://doi.org/10.1111/j.1467-7687.2011.01080.x.

Lyons, I. M., D. Ansari, and S. L. Beilock. 2015. "Qualitatively Different Coding of Symbolic and Nonsymbolic Numbers in the Human Brain." *Human Brain Mapping* 36, no. 2: 475–488. https://doi.org/10.1002/hbm.22641.

Maldjian, J. A., P. J. Laurienti, R. A. Kraft, and J. H. Burdette. 2003. "An Automated Method for Neuroanatomic and Cytoarchitectonic Atlas-Based Interrogation of fMRI Data Sets." *NeuroImage* 19, no. 3: 1233–1239. https://doi.org/10.1016/S1053-8119(03)00169-1.

Matejko, A. A., and D. Ansari. 2017. "How Do Individual Differences in Children's Domain Specific and Domain General Abilities Relate to Brain Activity Within the Intraparietal Sulcus During Arithmetic? An fMRI Study." *Human Brain Mapping* 38, no. 8: 3941–3956. https://doi.org/10.1002/hbm.23640.

McClelland, J. L., B. L. McNaughton, and R. C. O'Reilly. 1995. "Why There Are Complementary Learning Systems in the Hippocampus and Neocortex: Insights From the Successes and Failures of Connectionist Models of Learning and Memory." *Psychological Review* 102, no. 3: 419–457. https://doi.org/10.1037/0033-295X.102.3.419.

Menon, V. 2015. "Arithmetic in the Child and Adult Brain." In *The Oxford Handbook of Numerical Cognition*, 502–530. Oxford University Press.

Merten, K., and A. Nieder. 2009. "Compressed Scaling of Abstract Numerosity Representations in Adult Humans and Monkeys." *Journal of Cognitive Neuroscience* 21, no. 2: 333–346. https://doi.org/10.1162/jocn.2008.21032.

Misaki, M., Y. Kim, P. A. Bandettini, and N. Kriegeskorte. 2010. "Comparison of Multivariate Classifiers and Response Normalizations for Pattern-Information fMRI." *NeuroImage* 53, no. 1: 103–118. https://doi.org/10.1016/j.neuroimage.2010.05.051.

Moyer, R. S., and T. K. Landauer. 1967. "Time Required for Judgements of Numerical Inequality." *Nature* 215, no. 5109: 1519–1520. https://doi.org/10.1038/2151519a0.

Mumford, J. A., T. Davis, and R. A. Poldrack. 2014. "The Impact of Study Design on Pattern Estimation for Single-Trial Multivariate Pattern Analysis." *NeuroImage* 103: 130–138. https://doi.org/10.1016/j.neuroimage.2014.09.026.

Mundy, E., and C. Gilmore. 2009. "Children's Mapping Between Symbolic and Nonsymbolic Representations of Number." *Journal of Experimental Child Psychology* 103, no. 4: 490–502.

Mussolin, C., A. De Volder, C. Grandin, X. Schlogel, M. C. Nassogne, and M. P. Noel. 2010. "Neural Correlates of Symbolic Number Comparison in Developmental Dyscalculia." *Journal of Cognitive Neuroscience* 22, no. 5: 860–874. https://doi.org/10.1162/jocn.2009.21237.

Nieder, A. 2004. "The Number Domain-Can We Count on Parietal Cortex?" *Neuron* 44, no. 3: 407–409. https://doi.org/10.1016/j.neuron.2004.10.020.

Nieder, A. 2005. "Counting on Neurons: The Neurobiology of Numerical Competence." *Nature Reviews Neuroscience* 6, no. 3: 177–190. https://doi.org/10.1038/nrn1626.

Nieder, A., and S. Dehaene. 2009. "Representation of Number in the Brain." *Annual Review of Neuroscience* 32, no. 1: 185–208. https://doi.org/10.1146/annurev.neuro.051508.135550.

Núñez-Peña, M. I., and M. Suárez-Pellicioni. 2014. "Less Precise Representation of Numerical Magnitude in High Math-Anxious Individuals: An ERP Study of the Size and Distance Effects." *Biological Psychology* 103: 176–183. https://doi.org/10.1016/j.biopsycho.2014.09.004.

Park, J., and E. M. Brannon. 2013. "Training the Approximate Number System Improves Math Proficiency." *Psychological Science* 24, no. 10: 2013–2019. https://doi.org/10.1177/0956797613482944.

Park, J., and E. M. Brannon. 2014. "Improving Arithmetic Performance With Number Sense Training: An Investigation of Underlying Mechanism." *Cognition* 133, no. 1: 188–200. https://doi.org/10.1016/j.cognition.2014.06.011.

Park, J., V. Bermudez, R. C. Roberts, and E. M. Brannon. 2016. "Non-Symbolic Approximate Arithmetic Training Improves Math Performance in Preschoolers." *Journal of Experimental Child Psychology* 152: 278–293. https://doi.org/10.1016/j.jecp.2016.07.011.

Park, Y., A. A. Viegut, and P. G. Matthews. 2021. "More Than the Sum of Its Parts: Exploring the Development of Ratio Magnitude Versus Simple Magnitude Perception." *Developmental Science* 24, no. 3: e13043. https://doi.org/10.1111/desc.13043.

Penn, D. C., K. J. Holyoak, and D. J. Povinelli. 2008. "Darwin's Mistake: Explaining the Discontinuity Between Human and Nonhuman Minds." *Behavioral and Brain Sciences* 31, no. 2: 109–130. https://doi.org/10.1017/S0140525X08003543.

Peters, E., P. Slovic, D. Västfjäll, and C. K. Mertz. 2008. "Intuitive Numbers Guide Decisions." *Judgment and Decision Making* 3, no. 8: 619–635. https://doi.org/10.1017/S1930297500001571.

Peters, L., and B. De Smedt. 2018. "Arithmetic in the Developing Brain: A Review of Brain Imaging Studies." *Developmental Cognitive Neuroscience* 30: 265–279. https://doi.org/10.1016/j.dcn.2017.05.002.

Piazza, M., P. Pinel, D. Le Bihan, and S. Dehaene. 2007. "A Magnitude Code Common to Numerosities and Number Symbols in Human Intraparietal Cortex." *Neuron* 53, no. 2: 293–305. https://doi.org/10.1016/j.neuron.2006.11.022.

Pica, P., C. Lemer, V. Izard, and S. Dehaene. 2004. "Exact and Approximate Arithmetic in an Amazonian Indigene Group." *Science* 306, no. 5695: 499–503. https://doi.org/10.1126/science.1102085.

Pinel, P., S. Dehaene, D. Riviere, and D. LeBihan. 2001. "Modulation of Parietal Activation by Semantic Distance in a Number Comparison Task." *NeuroImage* 14, no. 5: 1013–1026. https://doi.org/10.1006/nimg.2001.0913.

Price, G. R., I. Holloway, P. Rasanen, M. Vesterinen, and D. Ansari. 2007. "Impaired Parietal Magnitude Processing in Developmental Dyscalculia." *Current Biology* 17, no. 24: R1042–R1043. https://doi.org/10.1016/j.cub.2007.10.013.

Qin, S., S. Cho, T. Chen, M. Rosenberg-Lee, D. C. Geary, and V. Menon. 2014. "Hippocampal-Neocortical Functional Reorganization Underlies Children's Cognitive Development." *Nature Neuroscience* 17, no. 9: 1263–1269.

Rothlein, D., J. DeGutis, and M. Esterman. 2018. "Attentional Fluctuations Influence the Neural Fidelity and Connectivity of Stimulus Representations." *Journal of Cognitive Neuroscience* 30, no. 9: 1209–1228. https://doi.org/10.1162/jocn_a_01306.

Rousselle, L., and M. P. Noel. 2007. "Basic Numerical Skills in Children With Mathematics Learning Disabilities: A Comparison of Symbolic vs Non-Symbolic Number Magnitude Processing." *Cognition* 102, no. 3: 361–395. https://doi.org/10.1016/j.cognition.2006.01.005.

Schneider, M., K. Beeres, L. Coban, et al. 2017. "Associations of Non-Symbolic and Symbolic Numerical Magnitude Processing With

Mathematical Competence: A Meta-Analysis." *Developmental Science* 20, no. 3: e12372. https://doi.org/10.1111/desc.12372.

Sekuler, R., and D. Mierkiewicz. 1977. "Children's Judgments of Numerical Inequality." *Child Development* 48, no. 2: 630–633. https://doi.org/10.2307/1128664.

Shirer, W. R., H. Jiang, C. M. Price, B. Ng, and M. D. Greicius. 2015. "Optimization of Rs-fMRI Pre-Processing for Enhanced Signal-Noise Separation, Test-Retest Reliability, and Group Discrimination." *NeuroImage* 117: 67–79. https://doi.org/10.1016/j.neuroimage.2015.05.015.

Theves, S., G. Fernandez, and C. F. Doeller. 2019. "The Hippocampus Encodes Distances in Multidimensional Feature Space." *Current Biology* 29, no. 7: 1226–1231. https://doi.org/10.1016/j.cub.2019.02.035.

Verguts, T., and F. Van Opstal. 2005. "Dissociation of the Distance Effect and Size Effect in One-Digit Numbers." *Psychonomic Bulletin & Review* 12, no. 5: 925–930. https://doi.org/10.3758/bf03196787.

Vigano, S., and M. Piazza. 2020. "Distance and Direction Codes Underlie Navigation of a Novel Semantic Space in the Human Brain." *Journal of Neuroscience* 40, no. 13: 2727–2736. https://doi.org/10.1523/JNEUROSCI.1849-19.2020.

Viganò, S., V. Rubino, A. D. Soccio, M. Buiatti, and M. Piazza. 2021. "Grid-Like and Distance Codes for Representing Word Meaning in the Human Brain." *NeuroImage* 232: 117876. https://doi.org/10.1016/j.neuroimage.2021.117876.

Vogel, S. E., C. Goffin, and D. Ansari. 2015. "Developmental Specialization of the Left Parietal Cortex for the Semantic Representation of Arabic Numerals: An fMR-Adaptation Study." *Developmental Cognitive Neuroscience* 12: 61–73. https://doi.org/10.1016/j.dcn.2014.12.001.

Weber, E. H. 1948. "Concerning Touch, 1834." In *Readings in the History of Psychology*, 155–156. Appleton-Century-Crofts.

Wei, W., H. Lu, H. Zhao, C. Chen, Q. Dong, and X. Zhou. 2012. "Gender Differences in Children's Arithmetic Performance Are Accounted for by Gender Differences in Language Abilities." *Psychological Science* 23, no. 3: 320–330. https://doi.org/10.1177/0956797611427168.

Wilkey, E. D., B. N. Conrad, D. J. Yeo, and G. R. Price. 2020. "Shared Numerosity Representations Across Formats and Tasks Revealed With 7 Tesla fMRI: Decoding, Generalization, and Individual Differences in Behavior." *Cerebral Cortex Communications* 1, no. 1: tgaa038. https://doi.org/10.1093/texcom/tgaa038.

Xia, M., J. Wang, and Y. He. 2013. "BrainNet Viewer: A Network Visualization Tool for Human Brain Connectomics." *PLoS One* 8, no. 7: e68910. https://doi.org/10.1371/journal.pone.0068910.

Zhang, D., L. Zhou, A. Yang, et al. 2023. "A Connectome-Based Neuromarker of Nonverbal Number Acuity and Arithmetic Skills." *Cerebral Cortex* 33, no. 3: 881–894. https://doi.org/10.1093/cercor/bhac108.

Zheng, L., Z. Gao, X. Xiao, Z. Ye, C. Chen, and G. Xue. 2018. "Reduced Fidelity of Neural Representation Underlies Episodic Memory Decline in Normal Aging." *Cerebral Cortex* 28, no. 7: 2283–2296. https://doi.org/10.1093/cercor/bhx130.

Supporting Information

Additional supporting information can be found online in the Supporting Information section.